NACA

RESEARCH MEMORANDUM

THE EFFECTS ON THE AERODYNAMIC CHARACTERISTICS OF VARYING THE WING THICKNESS RATIO OF A TRIANGULAR WING-BODY CONFIGURATION AT TRANSONIC SPEEDS FROM TESTS BY THE NACA WING-FLOW METHOD

By Albert W. Hall and James M. McKay

Langley Aeronautical Laboratory
Langley Field, Va.

NATIONAL ADVISORY COMMITTEE
FOR AERONAUTICS

WASHINGTON
April 2, 1952

Classification cancelled (or changed to) Unclassified

By Authority of NASA Tech Announcement

(OFFICER AUTHORIZED TO CHANGE)

74 30 Nov 54

By

GRADE OF OFFICER MAKING CHANGE

14 Feb 61

DATE

NATIONAL ADVISORY COMMITTEE FOR AERONAUTICS

RESEARCH MEMORANDUM

THE EFFECTS ON THE AERODYNAMIC CHARACTERISTICS OF VARYING THE WING THICKNESS RATIO OF A TRIANGULAR WING-BODY CONFIGURATION AT TRANSONIC SPEEDS FROM TESTS BY THE NACA WING-FLOW METHOD

By Albert W. Hall and James M. McKay

SUMMARY

Tests were made by the NACA wing-flow method at Mach numbers from 0.75 to 1.07 to determine the aerodynamic characteristics of three triangular wing-fuselage models which differed only in wing thickness-chord ratio. All three wings had an aspect ratio of 2.31 with 6-, 9-, and 12-percent-thick biconvex sections and the fuselage had a fineness ratio of 12.

Measurements were made of normal force, chord force, and pitching moment for various angles of attack. The Reynolds number of the tests was approximately 1.5×10^6 based on the mean aerodynamic chord of the model wing.

The effects of increasing wing thickness on the lift and pitching-moment characteristics were most pronounced at lift coefficients near zero and at Mach numbers below 1.0. For these conditions there was a marked decrease in the lift-curve slope as the wing thickness increased, particularly from 9 to 12 percent, and there was a much greater variation in aerodynamic-center position with Mach number. At Mach numbers of 1.0 and greater or at higher lift coefficients (about 0.3) the effects of wing thickness were relatively small. The variation of zero-lift drag with wing thickness through the Mach number range of these tests showed reasonable correlation with the transonic similarity law. Drag due to lift appeared to be very little affected by the variations in thickness and Mach numbers.

INTRODUCTION

As part of a program to determine the effect of wing section, plan form, and thickness on the aerodynamic characteristics of triangular wings at transonic and low-supersonic speeds, several wing-fuselage models have been tested by the NACA wing-flow method. Previous reports have presented the effect of section shape on the aerodynamic characteristics of two triangular wings (reference 1), the effect of reversing a triangular wing on a fuselage (reference 2), and the aerodynamic characteristics of two triangular wing-fuselage models at a Mach number of 1.25 (reference 3). The present paper presents the aerodynamic characteristics at transonic speeds of three wing-fuselage models differing only in wing thickness-chord ratio. The three models had triangular wings of aspect ratio 2.31 with 6-, 9-, and 12-percent-thick biconvex sections. Measurements were made of normal force, chord force, and pitching moment at various angles of attack through a Mach number range of 0.75 to 1.07.

SYMBOLS

M_L	local Mach number at surface of test section
M	effective Mach number at wing of model
q	effective dynamic pressure at wing of model, pounds per square foot
R	Reynolds number based on mean aerodynamic chord of model
α	angle of attack of model wing, degrees
ϵ	half apex angle of model wing, degrees
S	semispan-wing area of model, square feet
b/2	span of model wing, inches
c	local wing chord of model, inches
$\bar{c}$	mean aerodynamic chord of model wing, inches $\left(\frac{\int_0^{b/2} c^2 dy}{\int_0^{b/2} c\, dy}\right)$

t/c	wing thickness-chord ratio $\left(\frac{\text{Maximum thickness}}{\text{Chord}}\right)$
y	spanwise coordinate, inches
L	lift, pounds
M	pitching moment about 50-percent-$\bar{c}$ point, inch-pounds
D	drag, pounds
C_L	lift coefficient (L/qS)
C_m	pitching-moment coefficient $(M/qS\bar{c})$
C_D	drag coefficient (D/qS)
C_{D_P}	pressure drag coefficient of wing alone
C_{D_o}	drag coefficient at zero lift
A	aspect ratio $(4 \tan \epsilon)$
$\frac{dC_L}{d\alpha}$	rate of change of lift coefficient with angle of attack
$\frac{\Delta C_D}{\Delta C_L{}^2}$	average ratio of increment of drag coefficient above minimum to square of the increment of lift measured from that corresponding to minimum drag coefficient $\left(\frac{C_D - C_{D_{min}}}{\left[C_L - \left(C_L \text{ at } C_{D_{min}}\right)\right]^2}\right)$
$\frac{dC_m}{dC_L}$	rate of change of pitching-moment coefficient with lift coefficient

APPARATUS AND TESTS

The tests were made by the NACA wing-flow method in which the model was mounted in a region of high-speed flow over the wing of a North American F-51D airplane.

The three models tested differed only in wing thickness, having triangular wings of aspect ratio 2.31 ($\epsilon = 30^{\circ}$) with 6-, 9-, and 12-percent-thick biconvex sections. The fuselage of each model was a half-body of revolution having a fineness ratio of 12 with its center line curved to fit the contour of the test section and was fitted with an end plate. The models were mounted about 1/16 inch (for low α tests) and 1/8 inch (for high α tests) above the surface of the test section and fastened to a strain-gage balance below the test section by means of a shank which passed through a hole in the test section. This difference in model height above the test surface was a result of the curvature of the model and test surface which made more clearance necessary for the model to oscillate to higher angles. The model and balance oscillated together; thus normal force, chord force, and pitching moment could be measured at various angles of attack. Details of the models are given in tables I and II and figures 1 and 2.

The chordwise distribution of local Mach number M_L along the airplane wing surface in the test region is shown in figure 3 for several values of airplane Mach number and lift coefficient. The effective Mach number M at the wing of the model is also shown for each curve. The local Mach number was determined from static-pressure measurements made with orifices flush with the surface in tests with the model removed. The vertical Mach number gradient was 0.009 per inch as determined from measurements made with a static-pressure tube located at various distances above the surface of the test section. The effective Mach number at the wing of the model was determined as an average Mach number over the wing area of the model. A more detailed discussion of the determination of effective Mach number and effective dynamic pressure q can be found in reference 4.

The angle of attack was determined from measurements of model angle and local flow angle. The local flow angle was determined by a free-floating vane mounted outboard of the model station as discussed in reference 4.

The tests were made during high-speed dives of the F-51D airplane. Continuous measurements were made of angle of attack, normal force, chord force, and pitching moment as M varied from 1.07 to 0.75 and as the model was oscillated through the angle-of-attack range. The models with the 6- and 9-percent-thick wings were oscillated through an

angle-of-attack range of -3° to 10°. Then the models with the 6- and 12-percent-thick wings were oscillated through an angle-of-attack range of -3° to 22° using a less sensitive strain-gage balance than was used for the low-angle tests. The Reynolds number range for the tests is shown in figure 4.

REDUCTION OF DATA

Lift, drag, and pitching-moment coefficients are based on the wing area extended to the fuselage center line as shown in figure 2. Pitching moments are referred to the 50-percent mean-aerodynamic-chord point.

Corrections have been applied to the drag data for the effect of buoyancy on the fuselage due to pressure gradients in the test region. Buoyancy effects on the wings were found to be negligible. No attempt has been made to correct the drag data for the effect of the fuselage end plate. Aeroelastic effects were considered negligible and no corrections were applied.

The basic data were reduced for several cycles, each cycle being a complete oscillation through the angle-of-attack range. The Mach number for each cycle was determined as the average effective Mach number M from the beginning to the end of the cycle. There were a number of cycles recorded while the Mach number varied from 1.07 to 0.75; hence the average M was very close to the M at the beginning or end of the cycle. These data in the basic form are given in figures 5, 6, and 7 for a few Mach numbers. These and other cycles were cross-plotted to show variations of the aerodynamic characteristics with M at constant lift coefficients.

RESULTS AND DISCUSSION

Lift Characteristics

The variation of lift coefficient C_L with angle of attack α is shown in figure 5 for representative subsonic, transonic, and low-supersonic Mach numbers. The lift curves for the high-angle tests of the 6- and 12-percent-thick wings indicate a break occurring around $\alpha = 15°$ and $\alpha = 14°$, respectively, for subsonic Mach numbers (M = 0.760 to 0.751). The lift coefficient at which this break occurs is approximately 0.2 lower for the 12-percent-thick wing than for the 6-percent-thick wing. This break smooths out as indicated by the curves for M approximately 1.00 and a complete stall occurs at angles of attack

of 20° to 22°. At subsonic speeds an inflection point is indicated (where lift-curve slope begins to increase) at low angles (3° to 6°) for each of the configurations tested and this inflection becomes more pronounced as the wing thickness t/c increases from 0.06 to 0.09 to 0.12. The inflections disappear as M approaches 1.00 and a smooth variation exists up to the stall (approximately 20° to 22°). The curves presented for the 6-percent-thick configuration tested through the low α range using a balance of higher sensitivity than that used for the high α tests indicate a lower lift-curve slope. There seems to be no explanation for this difference other than the use of different balances to measure the forces.

The variation of α with M at constant values of C_L is shown in figure 8 for the three configuations tested. These curves show a break which increases in intensity as the wing t/c increases, and the Mach number at which this break occurs decreases as the wing t/c increases from 0.06 to 0.09 to 0.12.

The variation of lift-curve slope $dC_L/d\alpha$ at $C_L = 0$ and $C_L = 0.3$ with M is shown in figure 9 for the three configurations tested. Also shown for $C_L = 0$ are calculated values of $dC_L/d\alpha$ obtained by the methods given in references 5 and 6 and test values of $dC_L/d\alpha$ for the 6- and 9-percent-thick configurations at $M = 1.25$ from reference 3.

The results for the $\frac{t}{c} = 0.06$ configuration, at $C_L = 0$, are in reasonable agreement with subsonic theory up to a value of $M = 0.975$. Results above $M = 1.00$ considered in conjunction with previous tests at $M = 1.25$ (reference 3) indicate a trend over this range similar to that for supersonic theory (reference 6) but the actual values are 15 to 20 percent less than the theoretical values.

For a given M at $C_L = 0$ the values of $dC_L/d\alpha$ decrease as the wing thickness increases, particularly between $\frac{t}{c} = 0.09$ and 0.12. The greatest difference occurs near $M = 0.90$ where $dC_L/d\alpha$ for the $\frac{t}{c} = 0.12$ wing is only 60 percent of that for the $\frac{t}{c} = 0.06$ wing. The differences in $dC_L/d\alpha$ become smaller between $M = 1.00$ and 1.07. At $C_L = 0.3$ the effect of thickness almost disappears at M below 0.90 although above $M = 1.00$ the effects of thickness are about the same as at $C_L = 0$.

DRAG CHARACTERISTICS

The variation of drag coefficient C_D with C_L for several Mach numbers is shown in figure 6 for the three wing-fuselage configuations. The variation of C_D with M at constant values of C_L is shown in figure 10 for the three configurations. The variation of drag coefficient at zero lift C_{D_o} with M for the three configurations shows a decrease in the drag-rise Mach number as t/c increases from 0.06 to 0.09 to 0.12. The C_{D_o} curves also indicate an increase in the amount of drag rise from subsonic to supersonic speeds as t/c increases. Due to limitations involved in the semispan test technique and the unknown effects of the test-section boundary layer and the effects of the end plate, the absolute values of C_D are probably incorrect but it is believed that the variations with M, the amount of drag rise, and the differences between each configuration are of the correct order.

The drag due to lift is represented by the factor $\frac{\Delta C_D}{\Delta C_L^2}$ and the variation of this factor with M is shown in figure 11 for the range of C_L from 0 to 0.3 for the three configurations. For the $\frac{t}{c} = 0.06$ configuration the variation is practically constant over the Mach number range tested and the variation is relatively small for the thicker wing. Throughout the Mach number range the values of $\frac{\Delta C_D}{\Delta C_L^2}$ are slightly lower for the $\frac{t}{c} = 0.12$ configuration than for the $\frac{t}{c} = 0.09$ configuration even though the values of $dC_L/d\alpha$ were greater for the $\frac{t}{c} = 0.09$ configuration than for the $\frac{t}{c} = 0.12$ configuration.

The results of a correlation of the zero-lift drag characteristics of the three configurations by an adaptation of transonic similarity laws are shown in figure 12. Actually the similarity laws were developed for potential flow and hence would not be expected to be rigorously applicable to the results of the present investigation or any investigation involving viscous flow. Despite this limitation it appeared desirable to determine how well the results could be correlated.

Use was made of one form of the law for finite wings as presented in reference 7 which deals primarily with straight wings, but it is

pointed out in reference 7 that the similarity laws for delta wings are by coincidence the same as for straight wings. In applying the similarity law to the present data, that part of the drag of the models due to fuselage, end plate, and skin friction on the wing had to be subtracted from the measured values (since the similarity relations apply only to the pressure drag of the wing alone). In the absence of direct measurements this drag correction shown in figure 12(a) was determined by a least-squares solution which involved the measured C_{D_o} and the similarity parameters for which a linear variation between $\frac{C_{D_P}}{\left(\frac{t}{c}\right)^{5/3}}$ and $\frac{1}{A\left(\frac{t}{c}\right)^{1/3}}$ was assumed (over the range of airfoil thicknesses used in the tests) at a constant value of the parameter $\frac{\sqrt{|M^2 - 1|}}{\left(\frac{t}{c}\right)^{1/3}}$. The average correction drag for several values of $\frac{\sqrt{|M^2 - 1|}}{\left(\frac{t}{c}\right)^{1/3}}$ determined by this method was combined with the drag rise determined by free-fall tests of a body having a thickness distribution similar to the fuselage used in the present tests. The drag correction determined by this method is not strictly correct, since it assumes that the viscous effects can also be correlated on the basis of similarity parameters. Some uncertainty may also be introduced by the drag rise used for the fuselage as obtained from free-fall data for considerably higher Reynolds numbers. The difference C_{D_P} between the measured C_{D_o} and the estimated correction drag coefficient is plotted in figure 12(b) as a variation of $\frac{C_{D_P}}{\left(\frac{t}{c}\right)^{5/3}}$ with $\frac{\sqrt{|M^2 - 1|}}{\left(\frac{t}{c}\right)^{1/3}}$ for the three wing thicknesses. According to the similarity laws the parameter $\frac{C_{D_P}}{\left(\frac{t}{c}\right)^{5/3}}$ should vary consistently with $\frac{1}{A\left(\frac{t}{c}\right)^{1/3}}$ for given values of $\frac{\sqrt{|M^2 - 1|}}{\left(\frac{t}{c}\right)^{1/3}}$. The present data used in this correlation apparently were not sufficiently accurate or extensive to establish any such consistent variation. In order to determine how well the drag coefficient could be predicted, even though the variation of $\frac{C_{D_P}}{\left(\frac{t}{c}\right)^{5/3}}$ with $\frac{1}{A\left(\frac{t}{c}\right)^{1/3}}$ was neglected for the range of values

of $\frac{1}{A\left(\frac{t}{c}\right)^{1/3}}$ of the present tests, a single curve was faired through the data (fig. 12(b)). The values of C_{D_o} were calculated from this faired curve for $\frac{t}{c} = 0.06$, 0.09, and 0.12 and are compared in figure 12(c) with corresponding experimental results. The comparison in figure 12(c) indicates a reasonable correlation despite the fact that by omission of the parameter $\frac{1}{A\left(\frac{t}{c}\right)^{1/3}}$ the analysis is effectively two-dimensional.

Pitching-Moment Characteristics

The variation of pitching-moment coefficient C_m with C_L at various Mach numbers is shown in figure 7 for the three configurations. The curves given at M near 0.75 and 0.92 for the $\frac{t}{c} = 0.06$ configuration show a nearly linear variation of C_m with C_L up to the stall, whereas the corresponding curves for the thicker wing configurations (9 and 12 percent thick) show a less stable variation at low values of C_L than at higher values of C_L. This tendency toward a more stable break is probably associated with the previously mentioned inflections in the lift curves given for the two thicker wing configurations at these lower Mach numbers. At higher Mach numbers (near M = 1.00 and 1.07) the variation of C_m with C_L is similar for all three configurations and has the opposite tendency compared to the variation at lower Mach numbers exhibited by the thicker wings (that is, more stable slope near $C_L = 0$).

The variation of C_m with M at constant values of C_L is shown in figure 13 for the three configurations. As was noted in the lift curves there is disagreement between the low-angle and high-angle tests of the $\frac{t}{c} = 0.06$ configurations. Although there is disagreement in the magnitude of the values of C_m at given values of C_L, the variation with M is similar for both tests.

The variation of aerodynamic-center location with M at $C_L = 0$ and $C_L = 0.3$ is given in figure 14 for the three configurations tested.

An effect of wing thickness on aerodynamic-center location at $C_L = 0$ is indicated for values of $M < 1.00$. For the $\frac{t}{c} = 0.06$ configuration the aerodynamic center moved rearward about 8 percent of the mean aerodynamic chord $\bar{c}$ as the Mach number varied from 0.75 to 1.00. For the thicker wing configurations $\left(\frac{t}{c} = 0.09 \text{ and } \frac{t}{c} = 0.12\right)$ there was an initial forward movement of the aerodynamic center of approximately 7 and 12 percent $\bar{c}$ followed by a rapid rearward movement of the aerodynamic center at M between 0.90 and 1.00 of 22 and 29 percent $\bar{c}$, respectively. At $M > 1.00$ the aerodynamic-center location was about the same for all configurations. At $C_L = 0.3$ the thickness of the wing had little effect on the aerodynamic-center position at any Mach number in the range tested.

CONCLUDING REMARKS

Tests have been made by the NACA wing-flow method at Mach numbers between 0.75 and 1.07 on three triangular wing-fuselage models which differed only in wing thickness-chord ratio. All three wings were of aspect ratio 2.31 with 6-, 9-, and 12-percent-thick biconvex sections and were mounted on a fuselage of fineness ratio 12.

The effects on the lift and pitching-moment characteristics of increasing wing thickness were most pronounced at lift coefficients near zero and at Mach numbers below 1.00. For these conditions there was a marked decrease in the lift-curve slope as the wing thickness increased, particularly from 9 to 12 percent. With increase in wing thickness, there was a much greater variation in aerodynamic-center position as the Mach number varied up to 1.00. At Mach numbers of 1.00 and greater or at higher lift coefficients (about 0.3) the effects of wing thickness were relatively small. The variation of zero-lift drag with wing thickness through the Mach number range of these tests showed reasonable correlation with the transonic similarity law. The variation of wing thickness or Mach number appeared to have little effect on drag due to lift.

Langley Aeronautical Laboratory
National Advisory Committee for Aeronautics
Langley Field, Va.

REFERENCES

1. Hall, Albert W., and McKay, James M.: Comparison of Airfoil Sections on Two Triangular-Wing-Fuselage Configurations at Transonic Speeds from Tests by the NACA Wing-Flow Method. NACA RM L51F01, 1951.

2. McKay, James M., and Hall, Albert W.: The Effects on the Aerodynamic Characteristics of Reversing the Wing of a Triangular Wing-Body Combination at Transonic Speeds as Determined by the NACA Wing-Flow Method. NACA RM L51H23, 1951.

3. Hall, Albert W., and Morris, Garland J.: Aerodynamic Characteristics at a Mach Number of 1.25 of a 6-Percent-Thick Triangular Wing and 6- and 9-Percent-Thick Triangular Wings in Combination with a Fuselage. Wing Aspect Ratio 2.31, Biconvex Airfoil Sections. NACA RM L50D05, 1950.

4. Johnson, Harold I.: Measurements of Aerodynamic Characteristics of a 35° Sweptback NACA 65-009 Airfoil Model with $\frac{1}{4}$-Chord Plain Flap by the NACA Wing-Flow Method. NACA RM L7F13, 1947.

5. DeYoung, John: Theoretical Additional Span Loading Characteristics of Wings with Arbitrary Sweep, Aspect Ratio, and Taper Ratio. NACA TN 1491, 1947.

6. Brown, Clinton E.: Theoretical Lift and Drag of Thin Triangular Wings at Supersonic Speeds. NACA Rep. 839, 1946. (Supersedes NACA TN 1183.)

7. Danforth, Edward C. B.: A Correlation of Experimental Zero-Lift Drag of Rectangular Wings with Symmetrical NACA 65-Series Airfoil Sections by Means of the Transonic Similarity Law for Wings of Finite Aspect Ratio. NACA RM L51G20, 1951.

TABLE I

Geometric Characteristics of Model Configurations

Fuselage:	
Section	Modified 65-series body of revolution
Length, in.	14.00
Maximum diameter at 50 percent length, in.	1.17
Fineness ratio	12
Wings:	
Section	Biconvex
Thickness ratio, percent chord	
Model 1	6
Model 2	9
Model 3	12
Aspect ratio	2.31
Semispan-wing area including projected area of wing in fuselage, sq in.	10.78
$\bar{c}$, in.	4.07
Dihedral, deg	0
Incidence, deg	0

TABLE II

ORDINATES FOR FUSELAGE

[All dimensions are in inches]

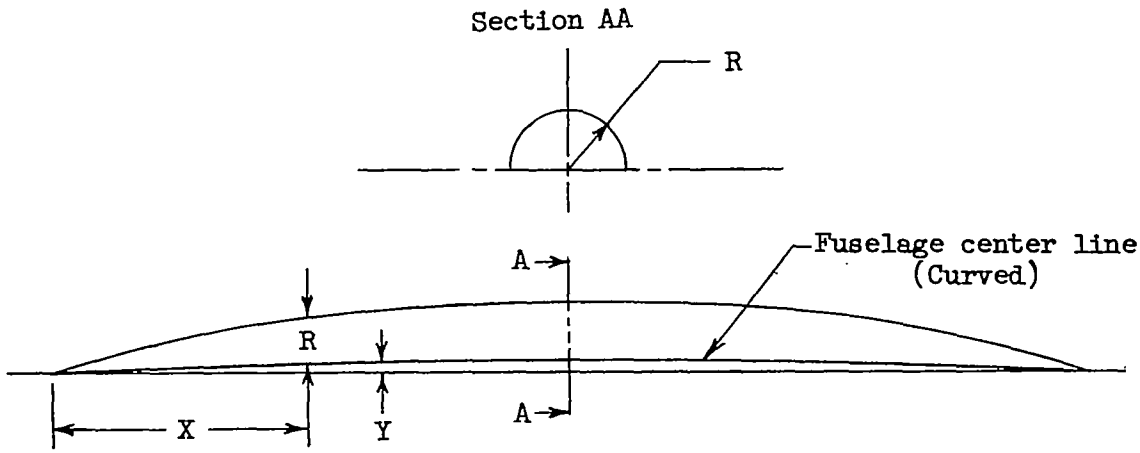

X	Y	R
0	0	0
.070	-----	.032
.105	.006	.042
.175	.011	.060
.350	.022	.101
.700	.042	.169
1.050	.059	.226
1.400	.075	.276
2.100	.102	.363
2.800	.124	.433
3.500	.140	.485
4.200	.153	.524
4.900	.160	.551

X	Y	R
5.600	0.169	0.569
6.300	.177	.580
7.000	.188	.583
7.700	.187	.578
8.400	.181	.563
9.100	.171	.538
9.800	.157	.499
10.500	.140	.438
11.200	.124	.354
11.900	.082	.267
12.600	.064	.178
13.300	.035	.089
14.000	0	0

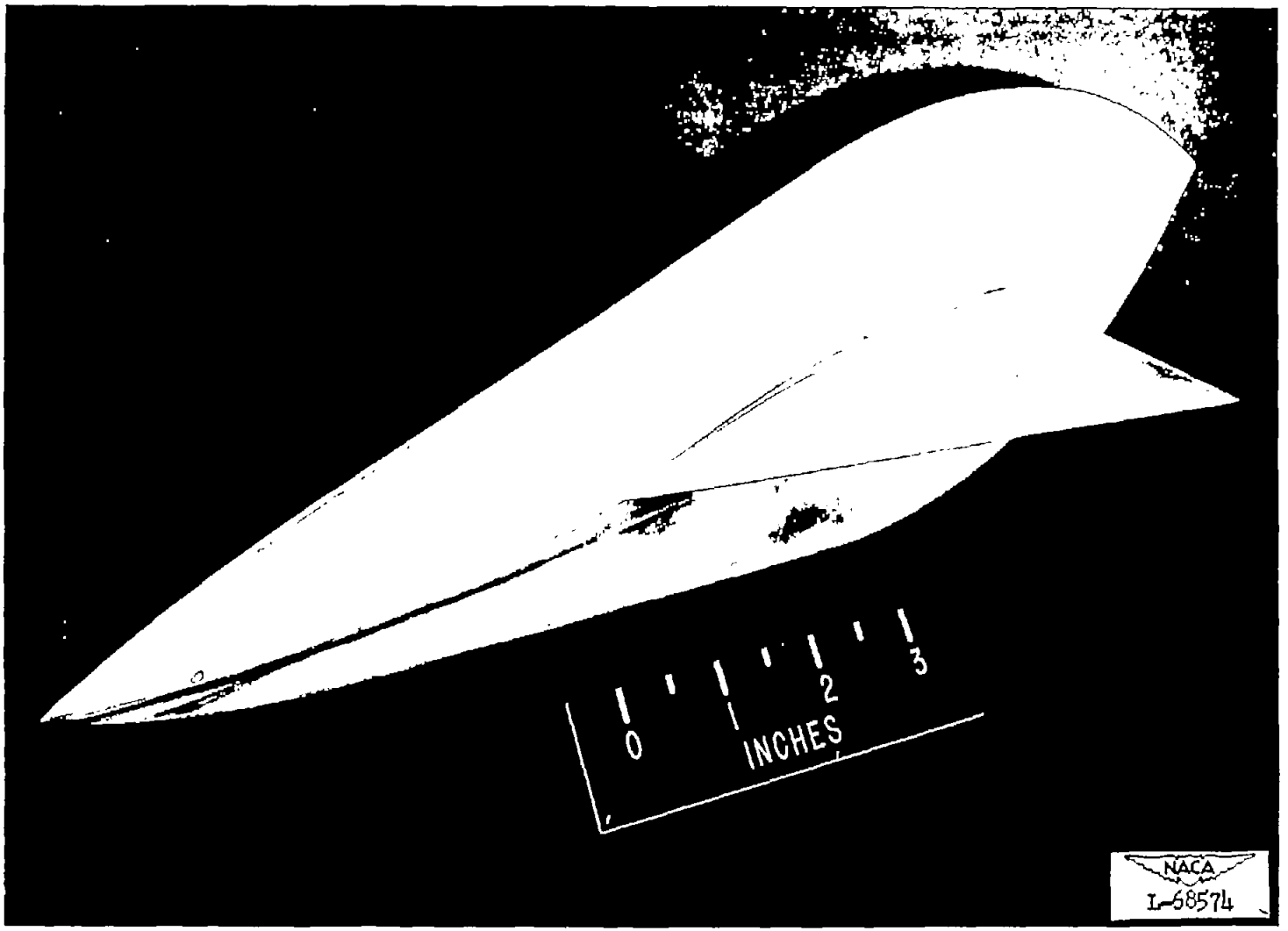

Figure 1.- Photograph of semispan wing-fuselage model and end plate.
A = 2.31; 9-percent-thick biconvex section.

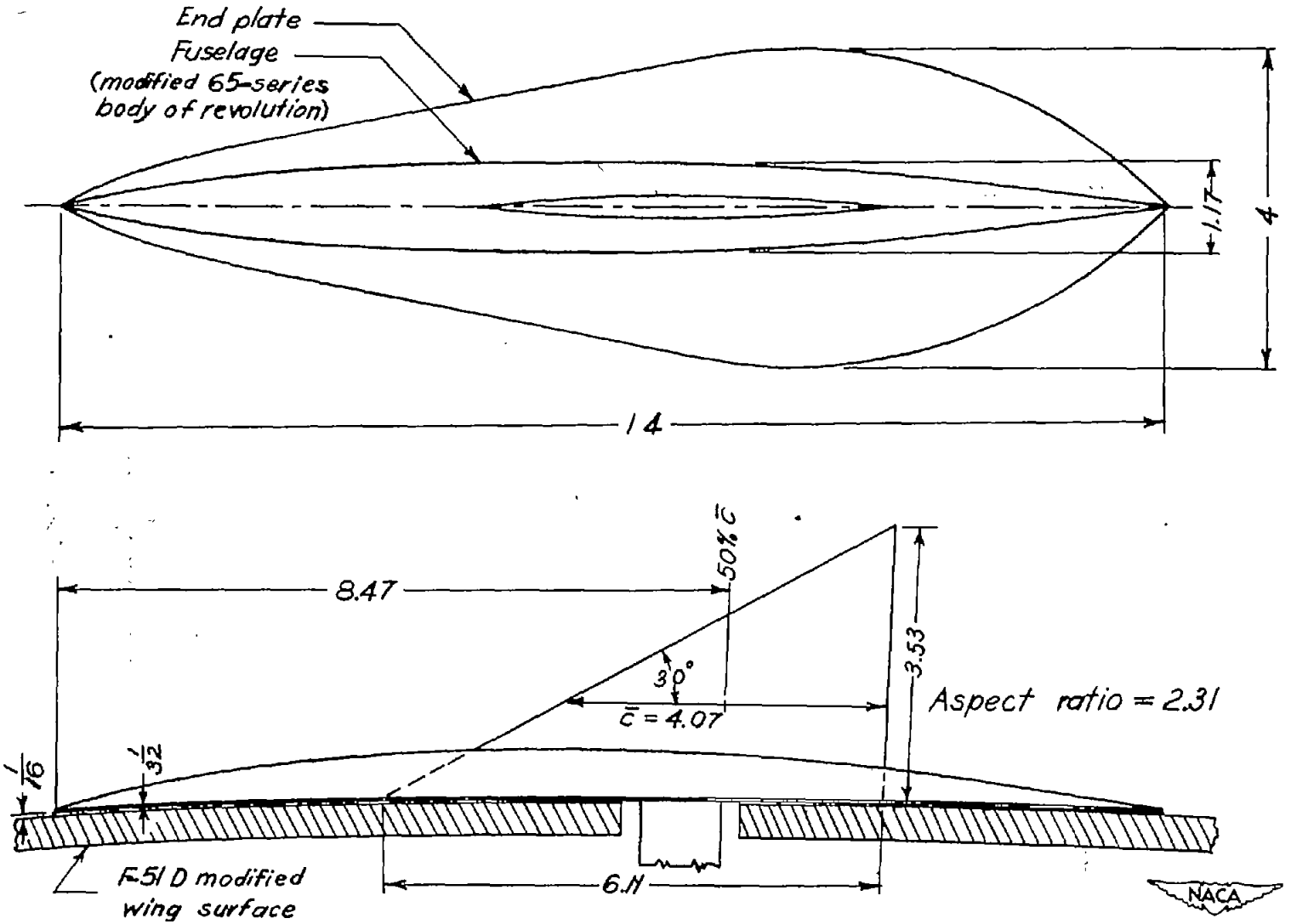

Figure 2.- Details of wing-fuselage model (all dimensions are in inches).

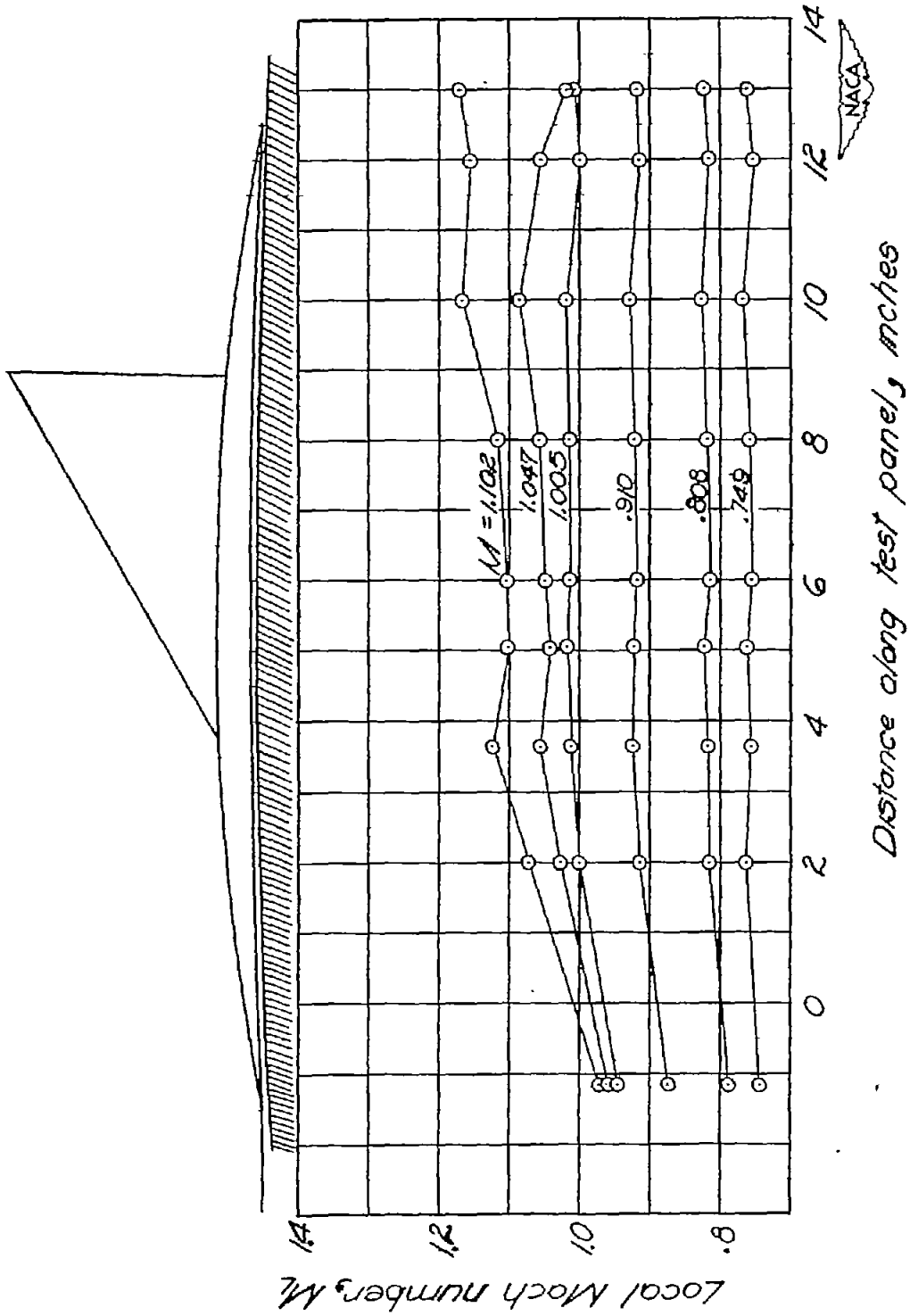

Figure 3.- Typical chordwise variation of Mach number in the test region on the surface of the airplane wing for several effective Mach numbers at the wing of the model. Chordwise location of model is also shown.

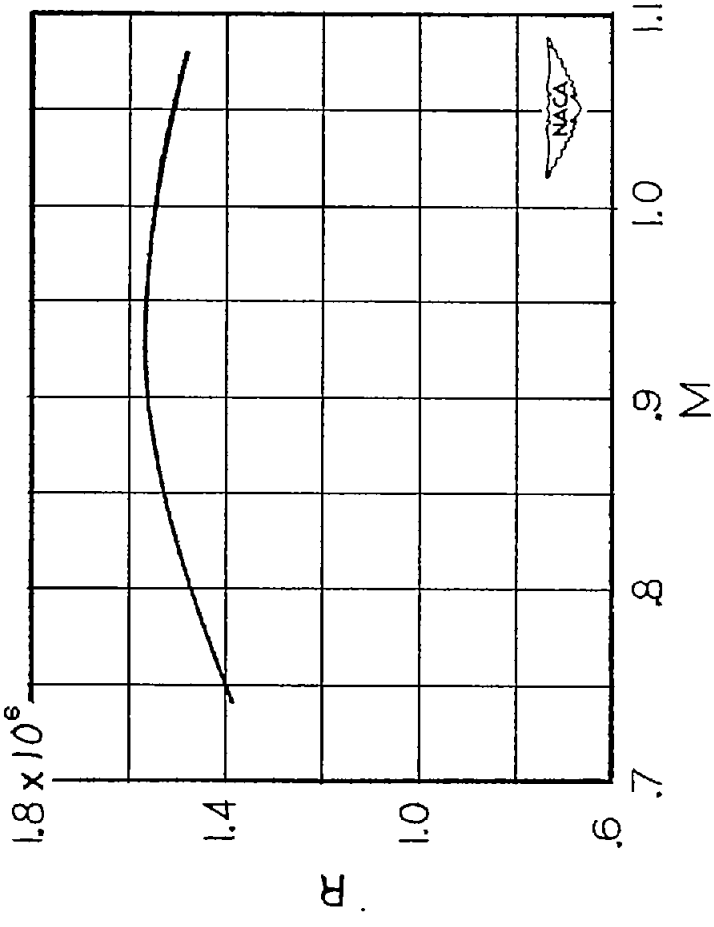

Figure 4.- Variation of test Reynolds number with effective Mach number.

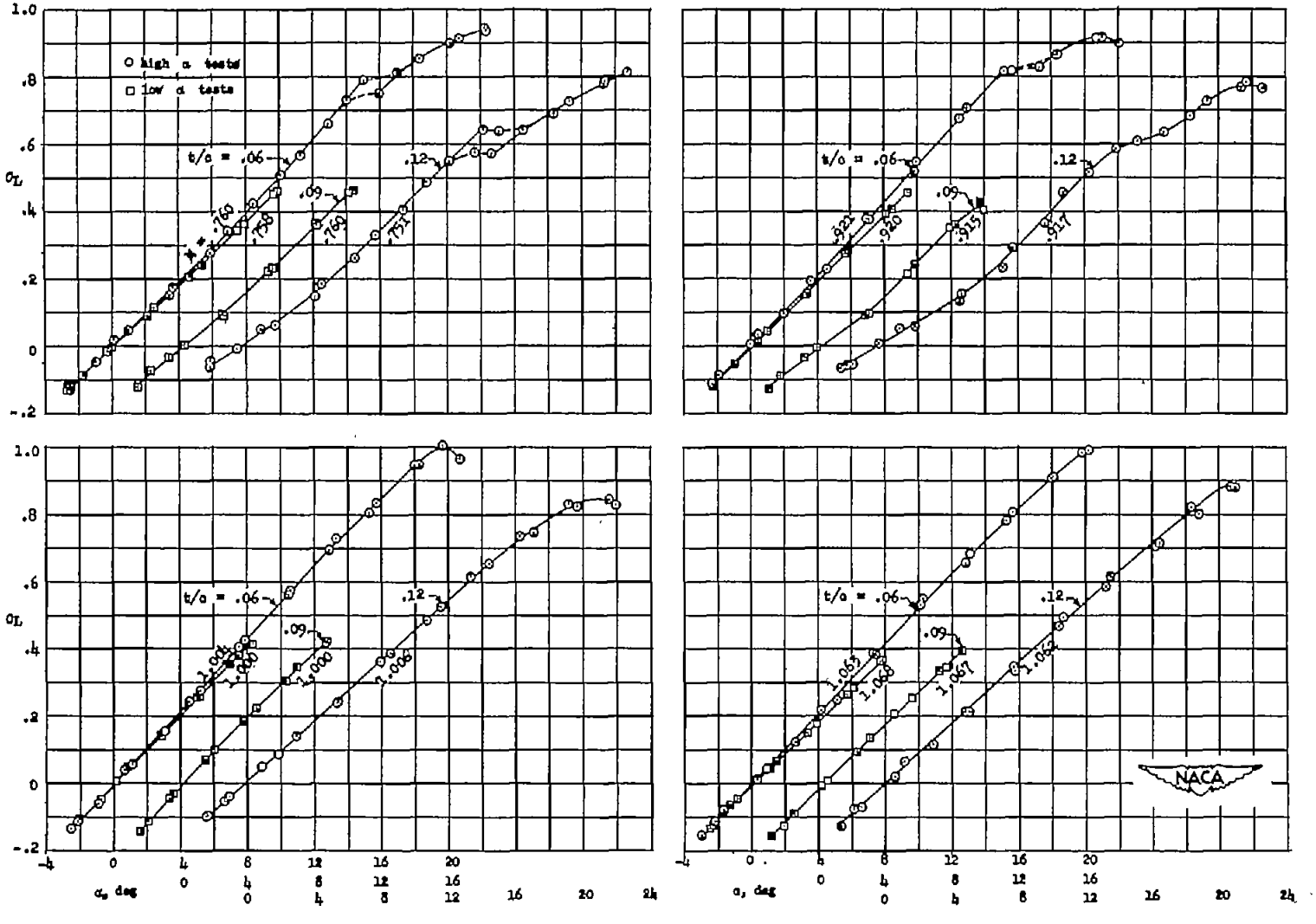

Figure 5.- Variation of lift coefficient with angle of attack for several Mach numbers for the configurations tested.

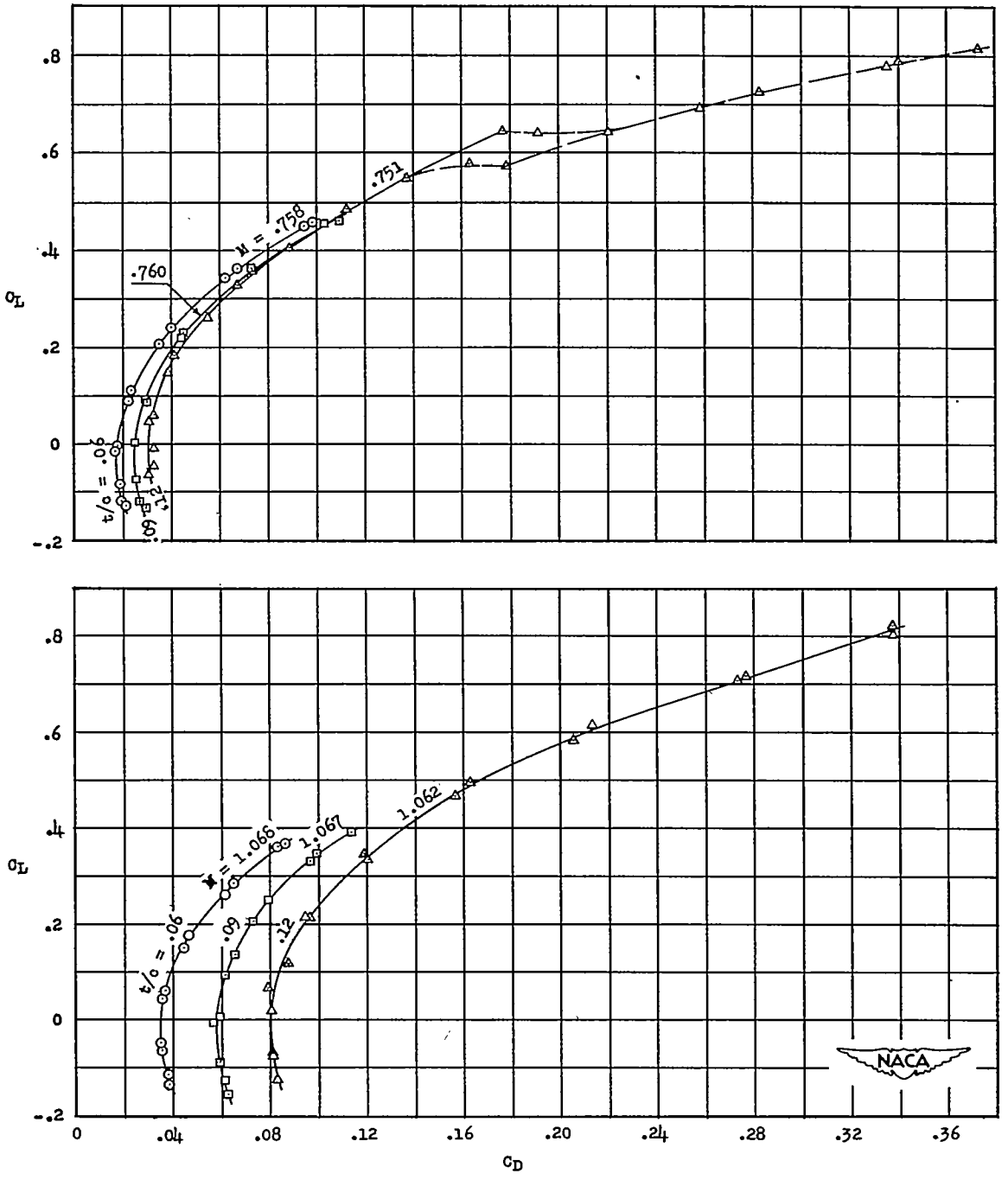

Figure 6.- Variation of drag coefficient with lift coefficient for several Mach numbers for the configurations tested.

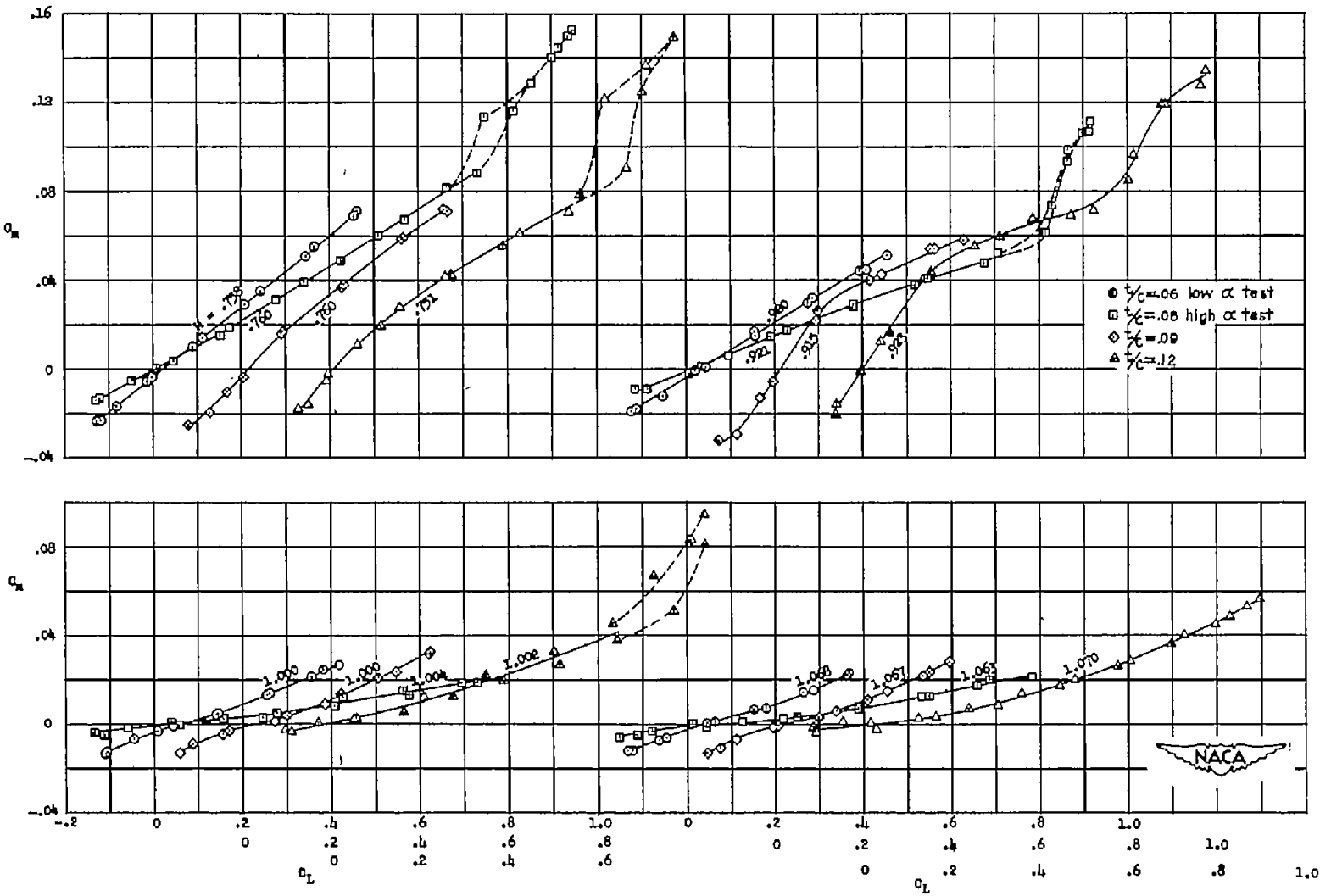

Figure 7.- Variation of pitching-moment coefficient with lift coefficient for several Mach numbers for the configurations tested.

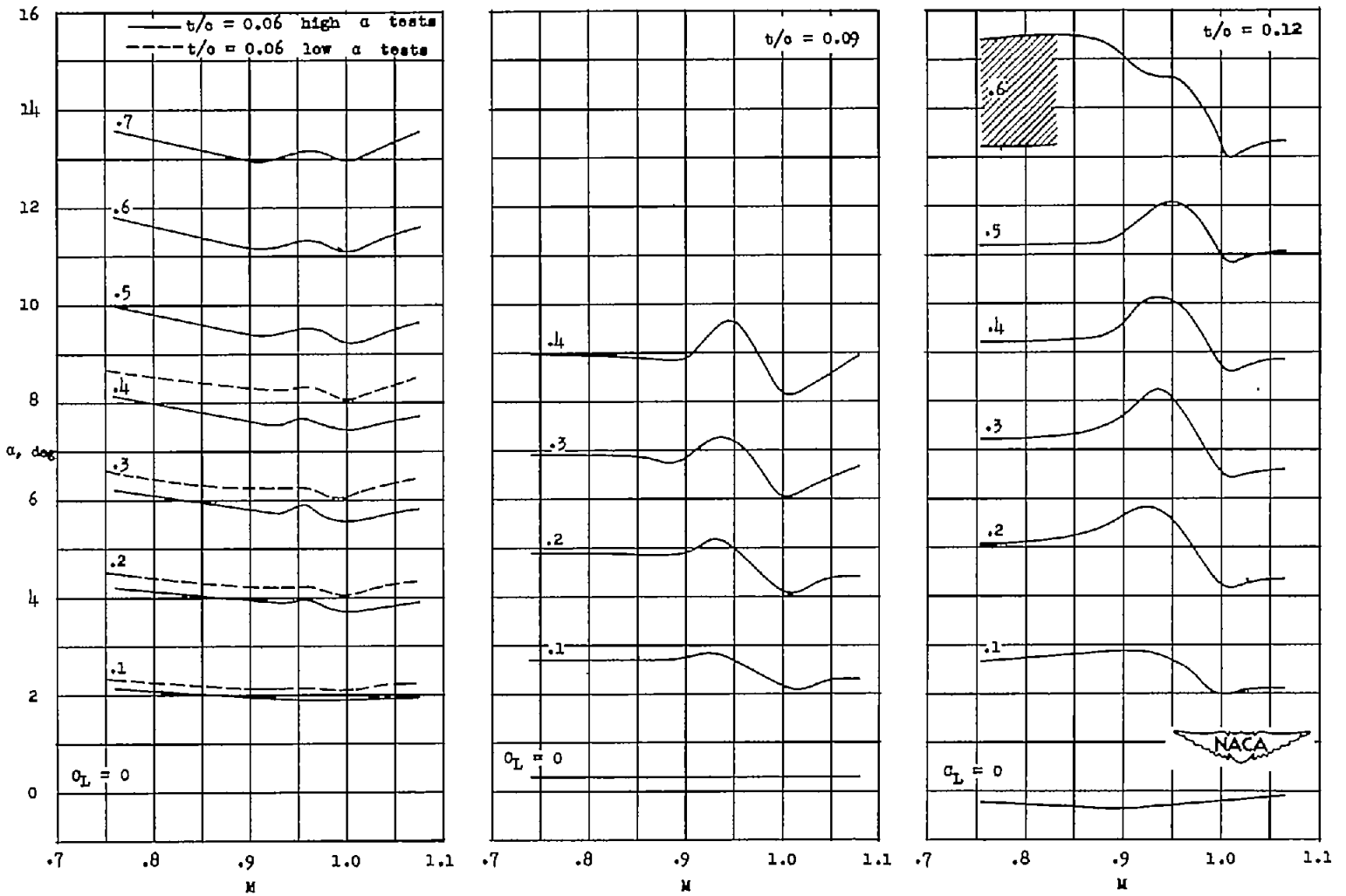

Figure 8.- Variation of angle of attack with Mach number at constant lift coefficient for the wing-fuselage models tested.

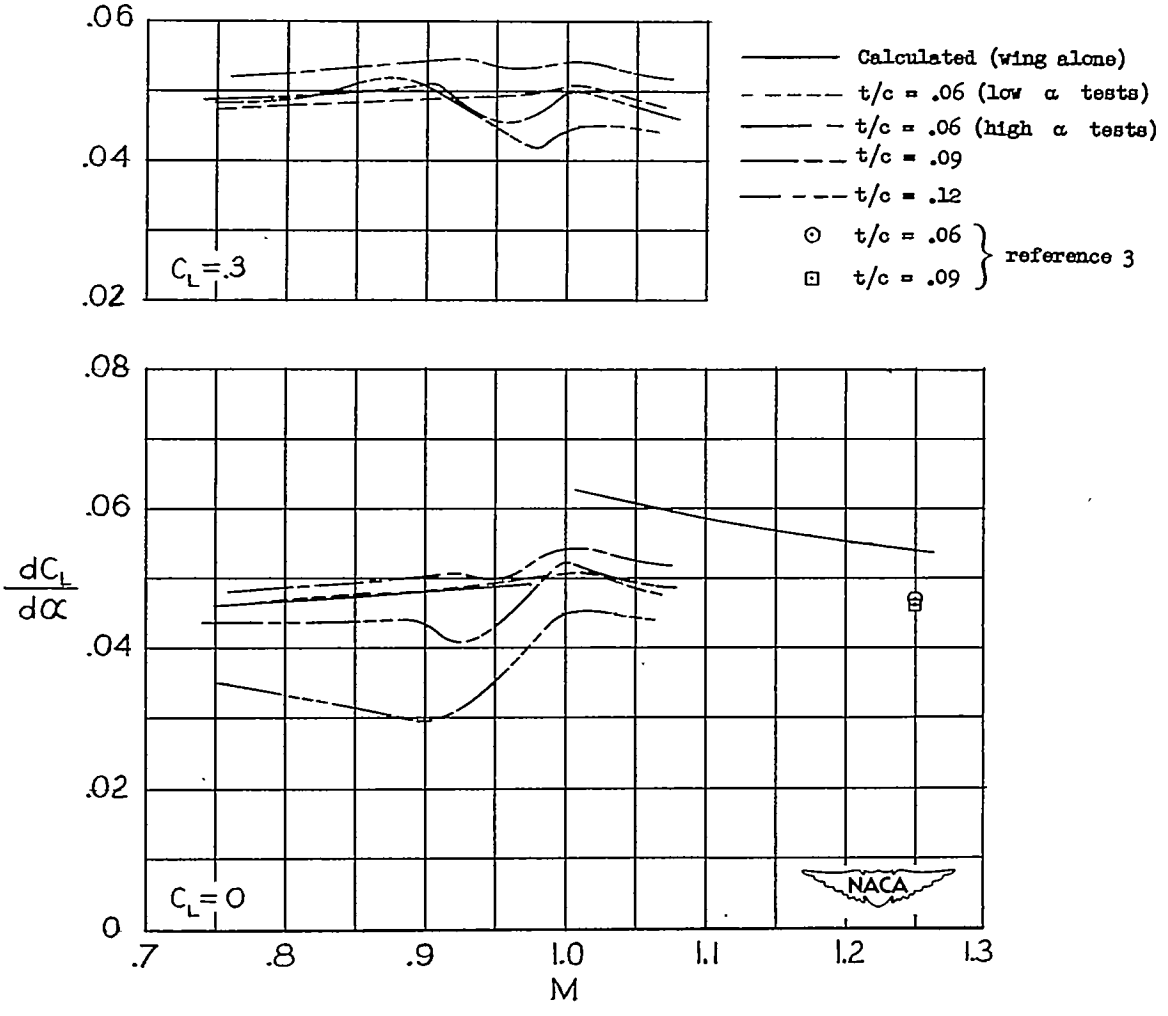

Figure 9.- Effect of Mach number on the lift-curve slope for various wing-fuselage configurations.

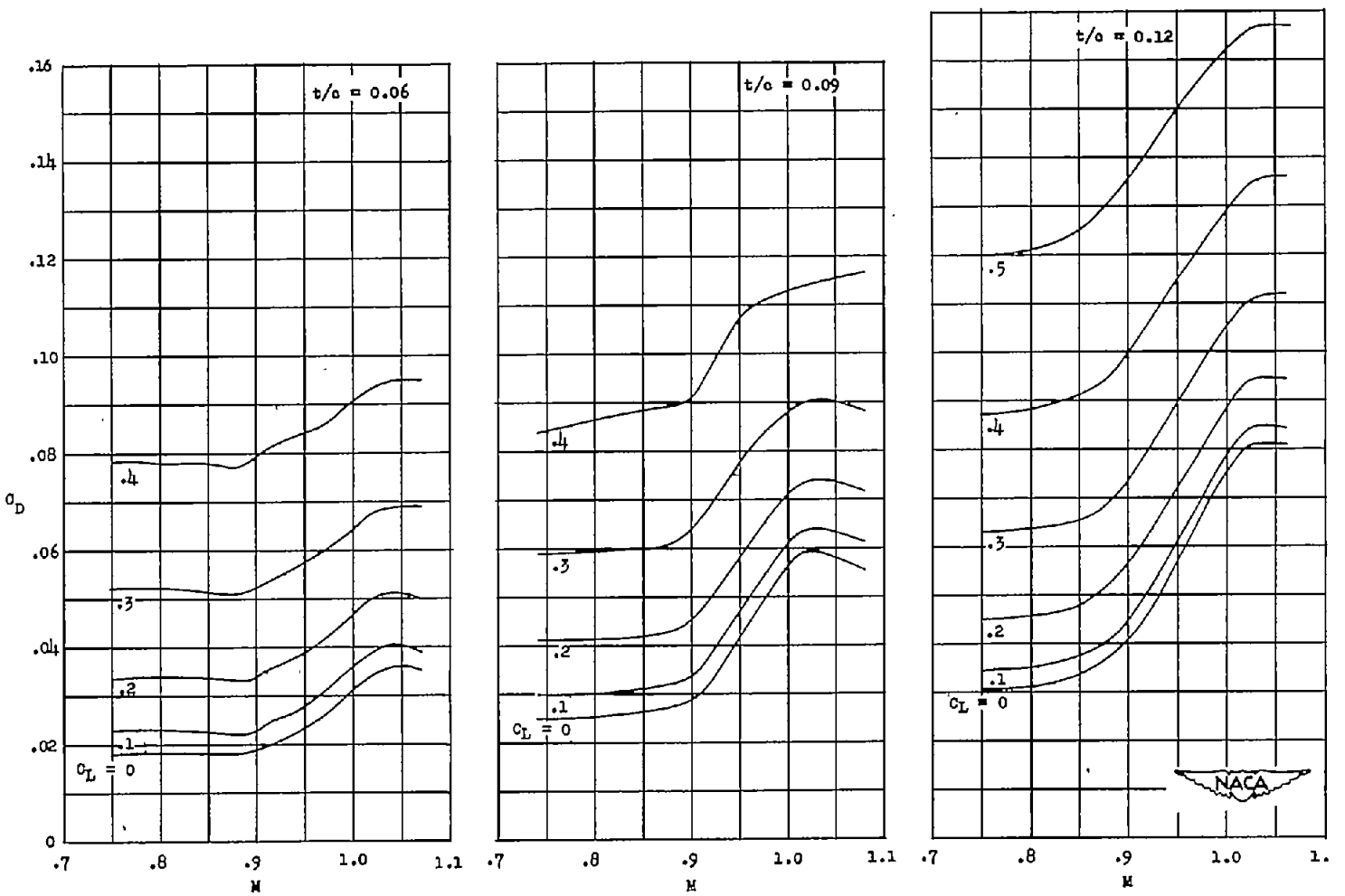

Figure 10.- Variation of drag coefficient with Mach number at constant lift coefficient for the wing-fuselage configurations tested.

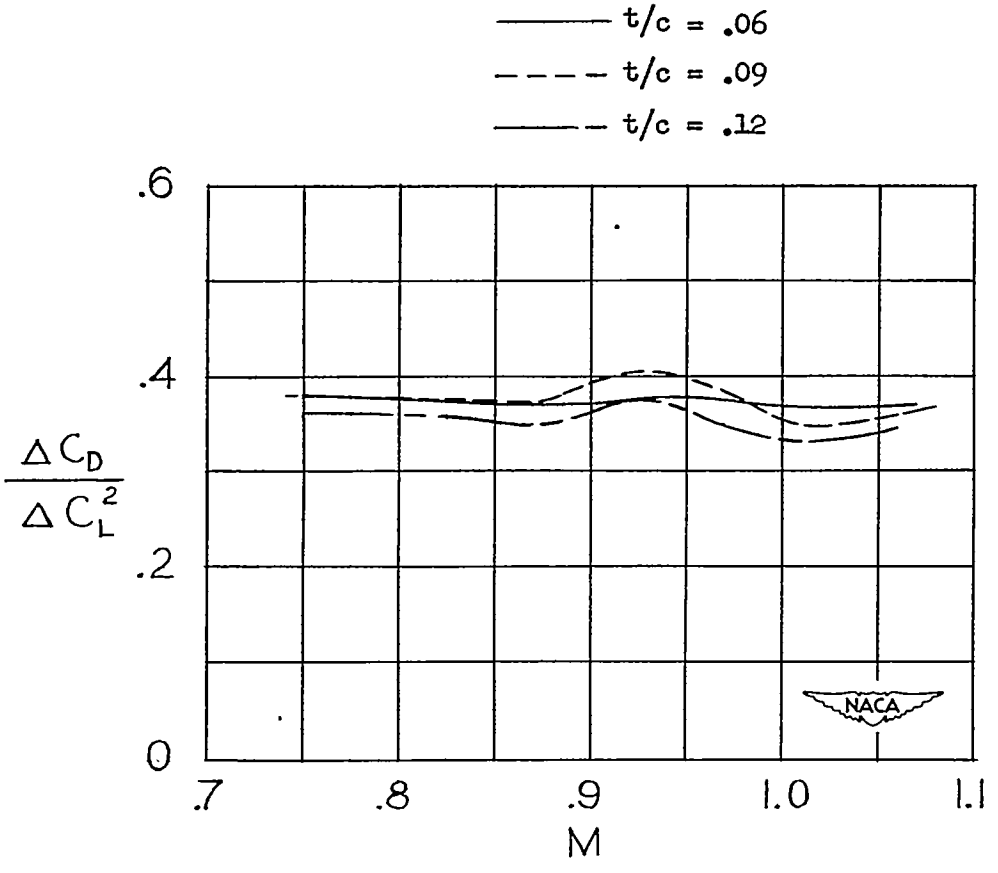

Figure 11.- Effect of Mach number on the factor $\frac{\Delta C_D}{\Delta C_L^2}$ for the wing-fuselage configurations tested. (C_L range from 0 to 0.3)

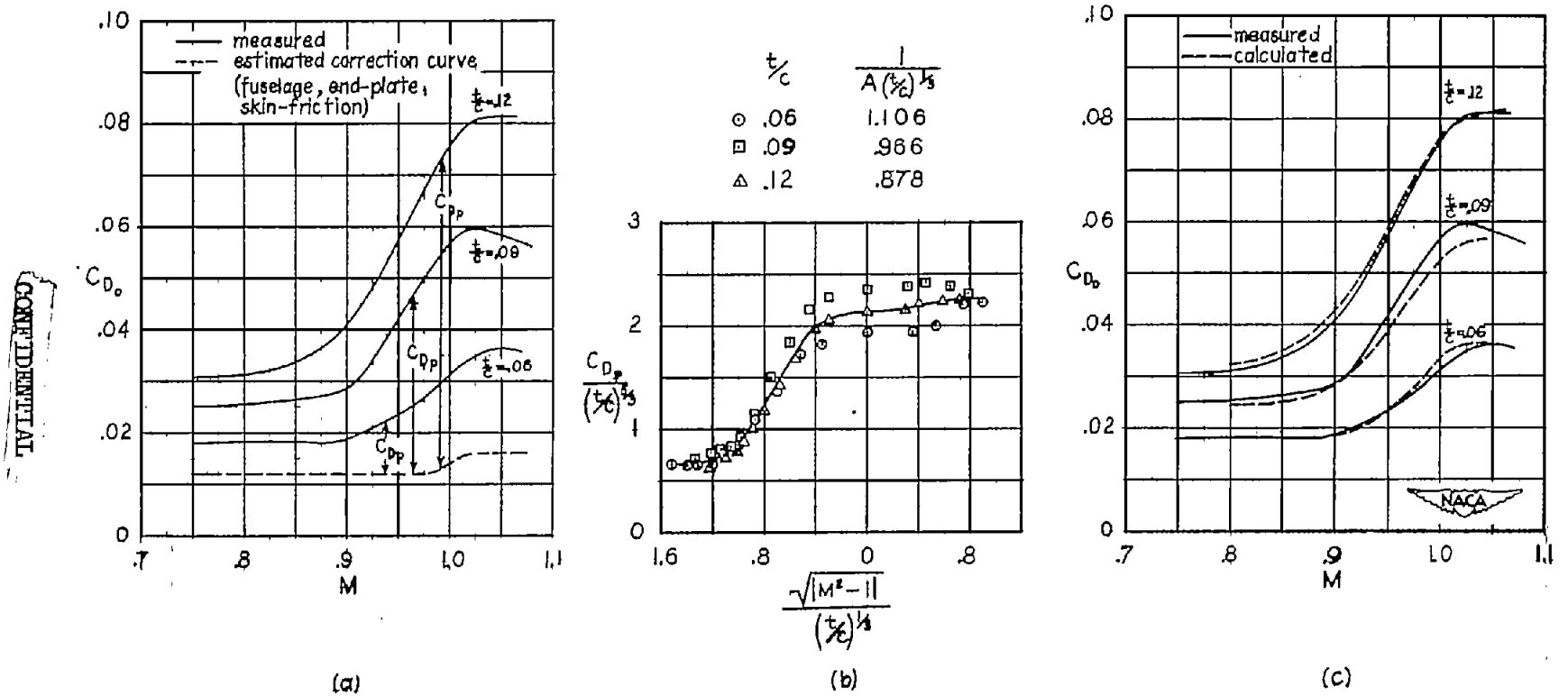

Figure 12.- Correlation of zero-lift drag data by the transonic similarity law.

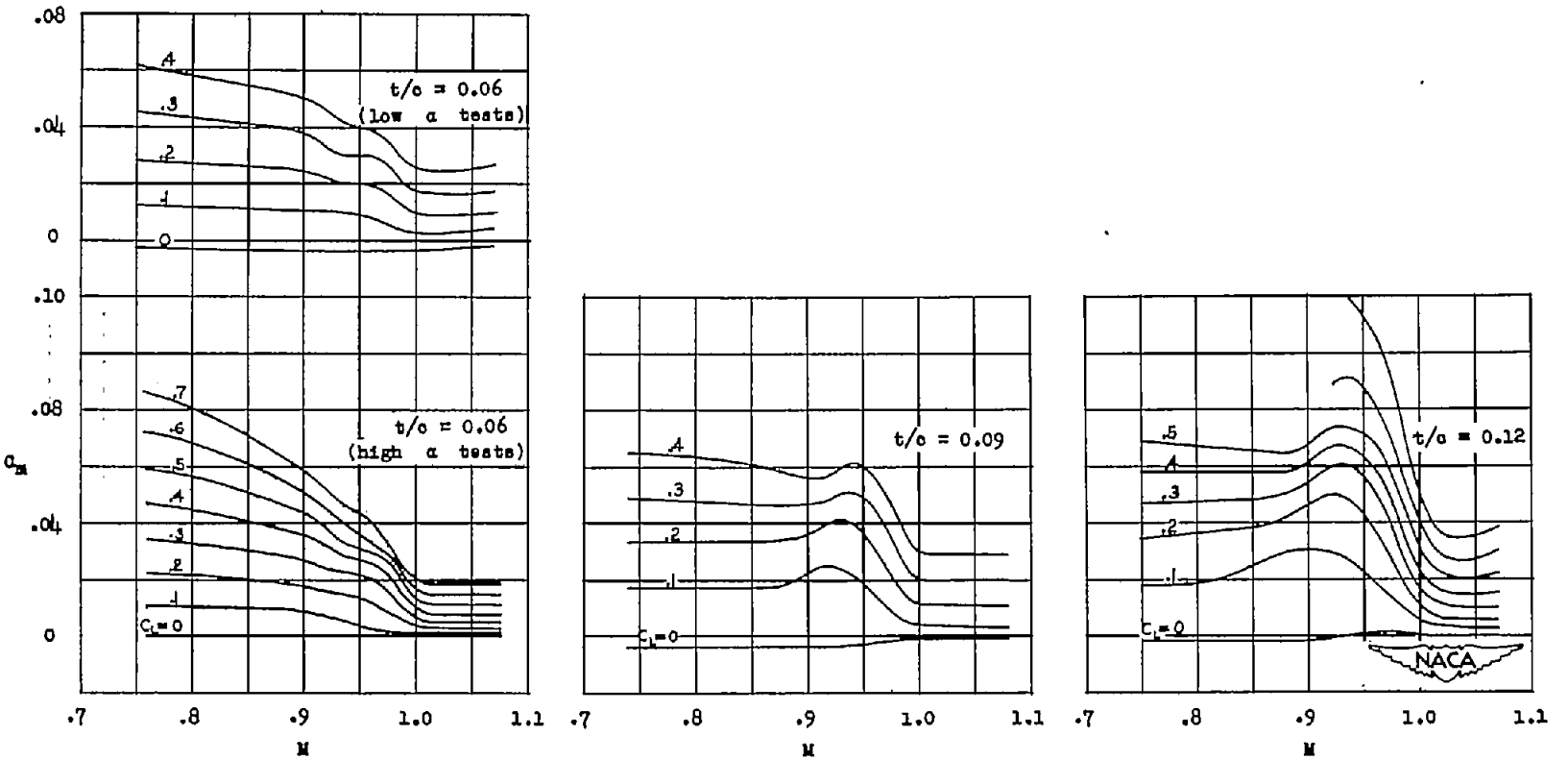

Figure 13.- Variation of pitching-moment coefficient with Mach number at constant lift coefficient for the wing-fuselage models tested.

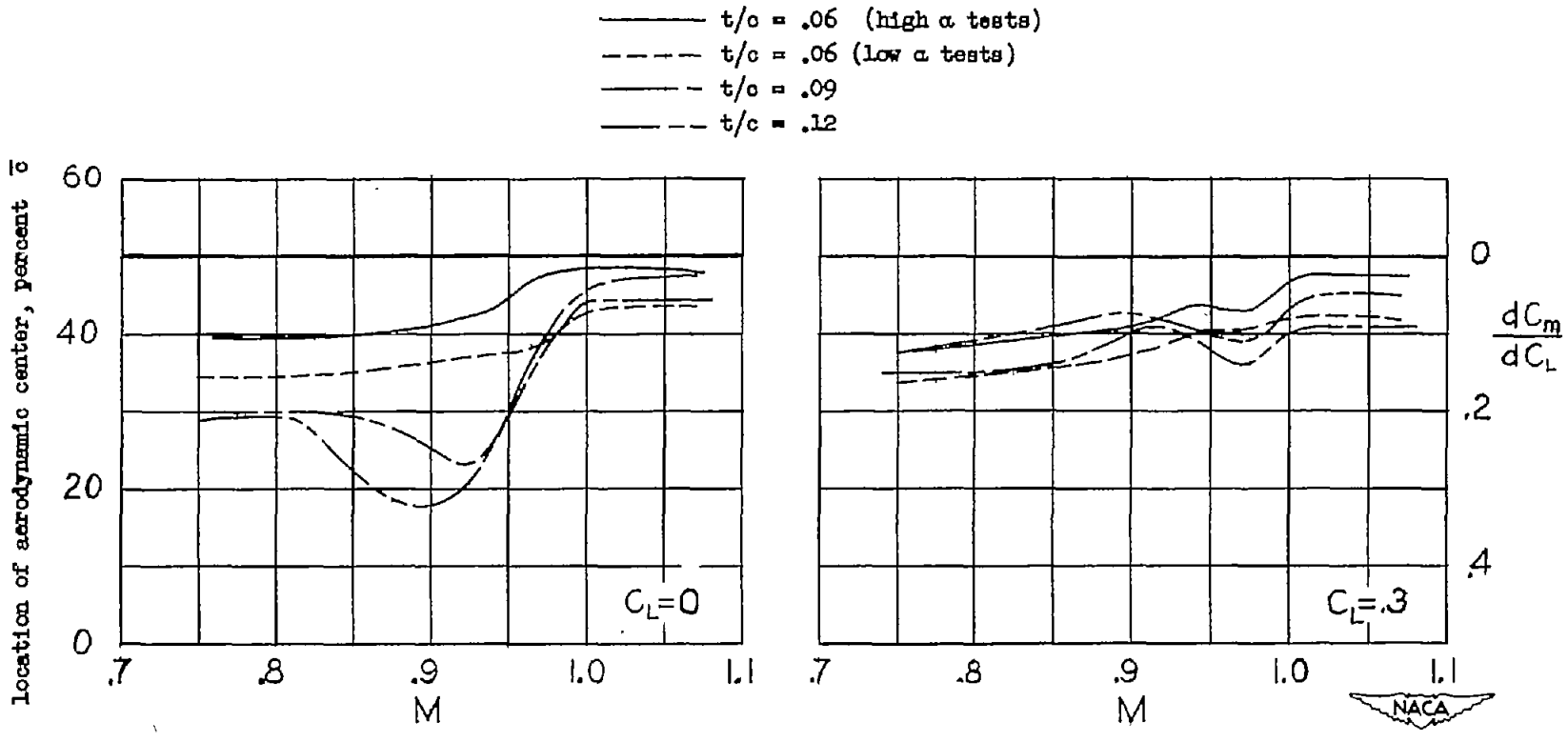

Figure 14.- Effect of Mach number on the location of the aerodynamic center.